

# LENGTH CONTROLLED IN-PLANE SYNTHESIS OF ALIGNED CARBON NANOTUBE ARRAY BY MICROMECHANICAL SPRING

Jungwook Choi, Soonjae Pyo, Jae-Ik Lee, and Jongbaeg Kim

School of Mechanical Engineering, Yonsei University, SOUTH KOREA

## ABSTRACT

We have demonstrated length-controllable in-plane synthesis of aligned carbon nanotube (CNT) array on microfabricated structures using micromechanical springs. The micromechanical spring provides precise compressive stress during the chemical vapor deposition process for CNT growth. Different loading results in different final length of the CNT array, as well as different alignment and defectiveness of the individual CNT. The length and the alignment of CNT array according to the spring stiffness were measured inside scanning electron microscope. The defectiveness of CNT was examined using micro-Raman spectroscopy, and the intensity ratio between D- and G-band was analyzed.

## INTRODUCTION

Remarkable mechanical, electrical and thermal properties of individual carbon nanotube (CNT) were studied previously [1-3]. Furthermore, researches on growth, properties, and applications of aligned CNT arrays were also reported. For the growth of aligned CNT arrays, thermal and plasma enhanced chemical vapor deposition (CVD) process were mainly used, and it exhibited interesting characteristics such as high porosity [4], large surface area [5], low mass density [6], and fatigue resistance on repeatable compression [7]. Based on their unique properties, the aligned CNT arrays were adopted as a functional material in various applications. The examples include multifunctional, low-noise and durable electrical brush [8, 9], wide range pressure sensor [10], high aspect ratio frame work [11], and electron source of field-emission device [12]. Recently, we demonstrated a process to integrate aligned CNT arrays on the sidewalls of silicon-processed microelectromechanical systems (MEMS). When two sets of aligned CNT arrays are synthesized within predefined gap, they make mechanical contact in the middle of the gap [13]. By using this self-adjusted growth of the CNT array, we reported CNT-integrated MEMS devices such as highly reliable and degradation-resistant micromechanical switch [14], contact time extended inertial switch [15], and torsional microactuator where CNT arrays were used as dry adhesive for high temperature fabrication process [16]. To extend the usage and to increase the controllability of aligned CNT arrays for practical applications, precise manipulation over the length and defectiveness of the synthesized CNTs is essential since they affect the properties of CNTs and therefore the functionalities of CNT-integrated devices. Numerous works have been performed to control the length of aligned CNT array including optimization of CVD parameters [17], timed synthesis while monitoring the growth rate of CNTs [18], and placing weight onto catalysts [19]. However, these methods were limited only to vertically aligned CNTs on planar substrate and required complex equipment.

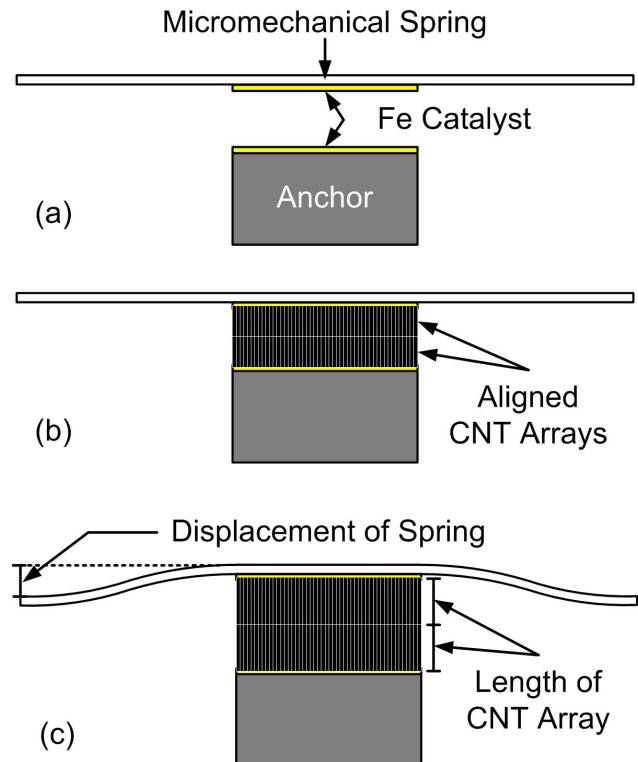


Figure 1: Detailed mechanism for length-controlled in-plane synthesis of the aligned CNT arrays. (a) The gap between micromechanical spring and anchor was isolated initially with iron catalyst on the sidewalls. (b) CNT arrays filled the gap during CVD process. (c) The micromechanical spring was deformed by extrusive growth force of the CNT arrays. According to the spring stiffness, the length of CNT arrays can be controlled.

Moreover, labor-intensive multiple steps of CVD process was required to obtain diverse length of CNT array. Alternatively, dependency of CNTs growth rate upon thickness of deposited gold were introduced [20], however the electrical short between adjacent patterns was unavoidable, which limits the employment of the method to practical CNT-based devices.

In this work, we developed and characterized the length-controllable and in-plane synthesis of aligned CNT arrays on MEMS by single CVD step. The compressive stress was applied perpendicularly on the aligned CNT arrays during the CVD process due to the buckling resistance of CNTs and the restoring force of the deformed micromechanical spring. As the spring stiffness increased, the length of CNT arrays decreased, and the morphology was changed to less-aligned state.

## DESIGN AND FABRICATION

The mechanism of length-controlled in-plane synthesis of aligned CNT arrays is explained in Figure 1. The anchor and the micromechanical spring were initially

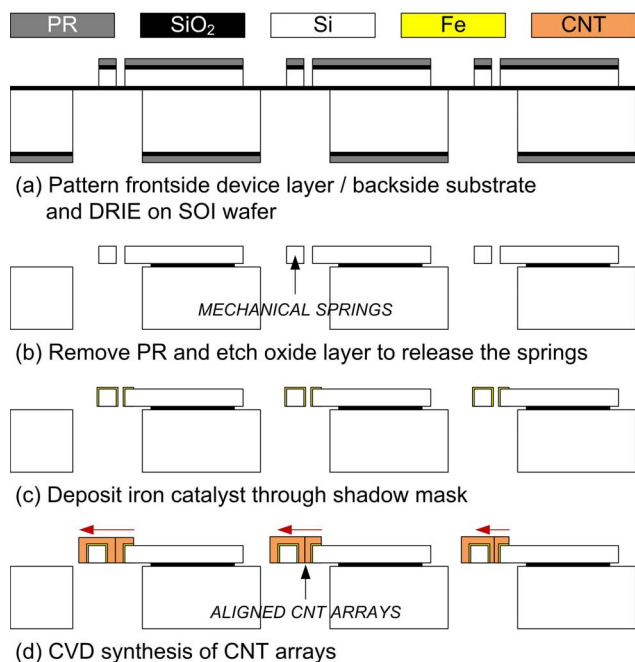


Figure 2: Fabrication process of the micromechanical spring and the aligned CNT arrays synthesis.

isolated with designed gap of 5  $\mu\text{m}$ , and the iron catalyst for CNT synthesis was deposited on the sidewalls of both anchor and spring. (Figure 1(a)). The gap was filled by the aligned CNT arrays during the CVD process, and the CNT arrays came in contact in the middle of the gap (Figure 1(b)). Once the gap was filled completely, extrusive growth force of the CNT array was delivered to the micromechanical spring. The two sets of CNT arrays did not penetrate into each other while the growth was in progress since high areal number density of CNTs and van der Waals force inside the CNT array inhibited overgrowth. As a result, the micromechanical spring was deformed during the CVD process (Figure 1(c)). Hence the applied compressive stress on the aligned CNT array was dependent on the spring stiffness, and this provided the length-tunability of CNT array when other CVD parameters were identical.

The fabrication process of the micromechanical springs and the anchors, and CVD synthesis of the CNT arrays are described in Figure 2. It started on silicon-on-insulator (SOI) wafer with a thickness of 20  $\mu\text{m}$  device layer, 2  $\mu\text{m}$  buried oxide layer, and 450  $\mu\text{m}$  substrate. Two thermal oxide layers of 1  $\mu\text{m}$  in thickness on both sides of SOI wafer were patterned and etched. Then the frontside silicon device layer and the backside substrate were sequentially etched by deep reactive ion etching (DRIE) with the thermal oxide layers as etch masks (Figure 2(a)). Remained photoresist was removed by piranha solution, and the thermal oxide and buried oxide layers were etched by hydrofluoric acid to release the micromechanical springs while the buried oxide underneath the anchor was maintained (Figure 2(b)). After the silicon processing, a shadow mask was aligned on top of the device layer, and 5 nm-thick iron catalyst was deposited selectively on the micromechanical spring and the edge of anchor through the opening holes of shadow mask (Figure 2(c)). Due to the imperfect directionality of

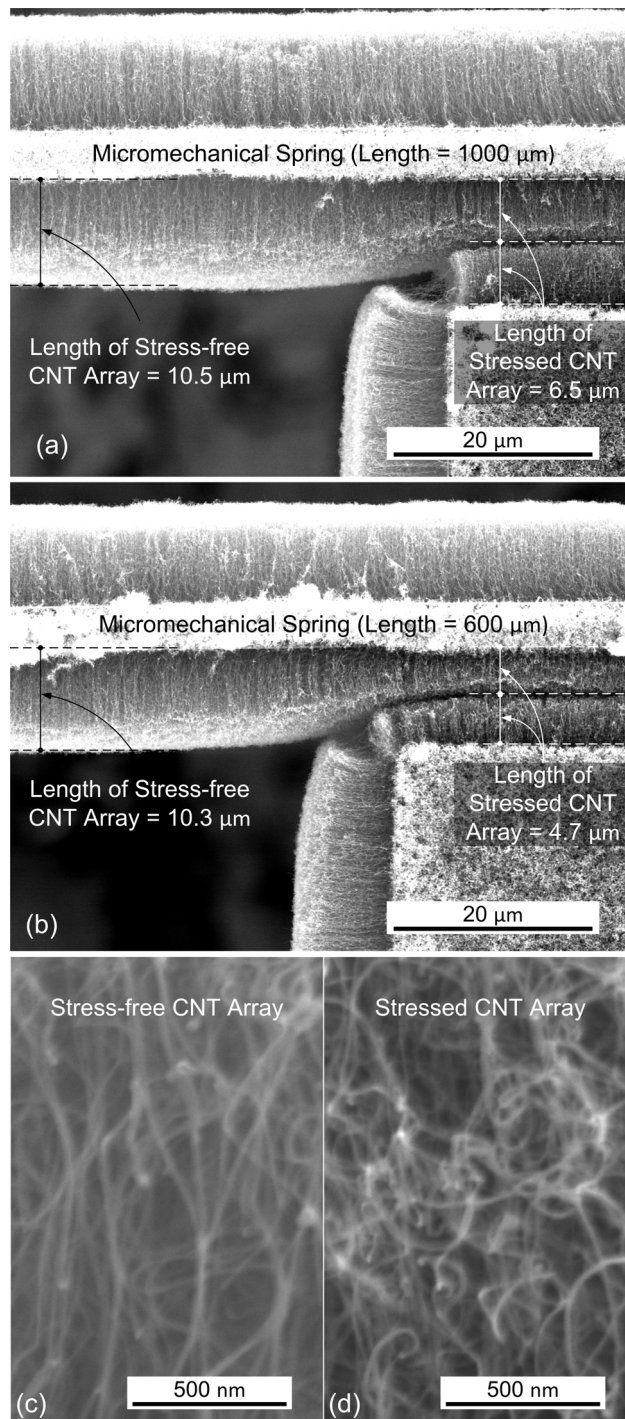


Figure 3: SEM images of the micromechanical spring with the integrated CNT arrays. The final length of CNT array grown under 6.7 N/m and 31.3 N/m of spring stiffness was (a) 6.5  $\mu\text{m}$  and (b) 4.7  $\mu\text{m}$ , and the length of stress-free CNT arrays was 10.5  $\mu\text{m}$  and 10.3  $\mu\text{m}$ , respectively. (c, d) The morphology of stressed CNT array during CVD process was less-aligned and buckled than stress-free CNT array.

metallization process, the iron catalyst was deposited on both the top surfaces and the sidewalls of microstructures. Finally, the CVD synthesis of CNT arrays was performed in a tube furnace. The furnace was pumped down to a base pressure below  $10^3$  Pa and purged with 100 sccm of nitrogen gas. When temperature reached to 700  $^\circ\text{C}$ , 100 sccm of ammonia gas was introduced for 30 min as a

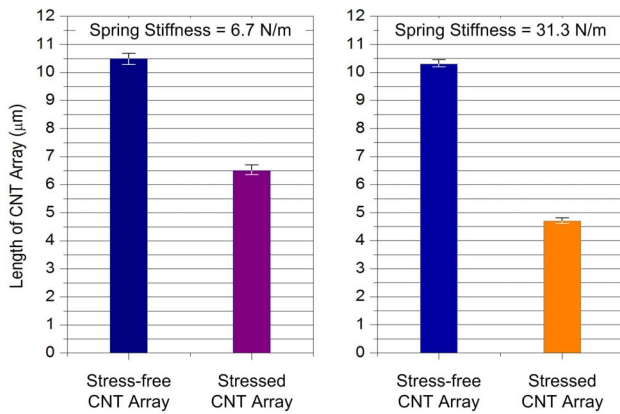


Figure 4: Length of the CNT array grown with compressive stress according to the spring stiffness. The length ratio with respect to the stress-free CNT array for 6.7 and 31.3 N/m of spring stiffness is 1.6 and 2.2, respectively.

pretreatment of the iron catalyst, and subsequently, acetylene gas as a carbon source was flowed for 15 min. It is noted that every CVD parameters were identical for the aligned CNT synthesis except the spring constant of the micromechanical spring for number of different test structures designed.

## RESULTS AND DISCUSSION

The results of the in-plane and the length-controlled synthesis of aligned CNT arrays are shown in scanning electron microscope (SEM) images of Figure 3. The designed width and height of micromechanical spring were 5 and 20 μm, and the length of spring was varied for different spring stiffness. In two cases of 1000 and 600 μm spring length, the length of aligned CNT array was 6.5 and 4.7 μm, respectively, as shown in Figure 3(a) and (b). Corresponding spring constants for the two cases are calculated to be 6.7 and 31.3 N/m based on fixed-fixed boundary condition and point load at the center of spring with silicon Young's modulus of 169 GPa in <110> direction. It is noteworthy that the length of CNT arrays grown without compressive stress was apparently much longer than the stressed CNT arrays. The length of stress-free CNT array was above 10 μm in both cases, and this can be observed in Figure 3(a) and (b). Furthermore, as shown in Figure 3(c) and (d), the CNTs stressed by the micromechanical spring during the growth process were rather entangled and collapsed compared to those grown without vertical load by spring. As a result, applied compressive stress during the CVD process induced buckling of the CNTs, and this influenced on the final length of the aligned CNT array. These experimental results are plotted in Figure 4. While the lengths of two cases of stress-freely grown CNT arrays were almost identical, the lengths of stressed CNT arrays were dependent on the stiffness of micromechanical springs. The length ratio between stress-free and stressed CNT arrays was 1.6 and 2.2 for the spring stiffness of 6.7 and 31.3 N/m, respectively.

The buckled and less-aligned morphology of CNTs observed in Figure 3(c) and (d) may affect defectiveness inside the individual CNT. This was confirmed by

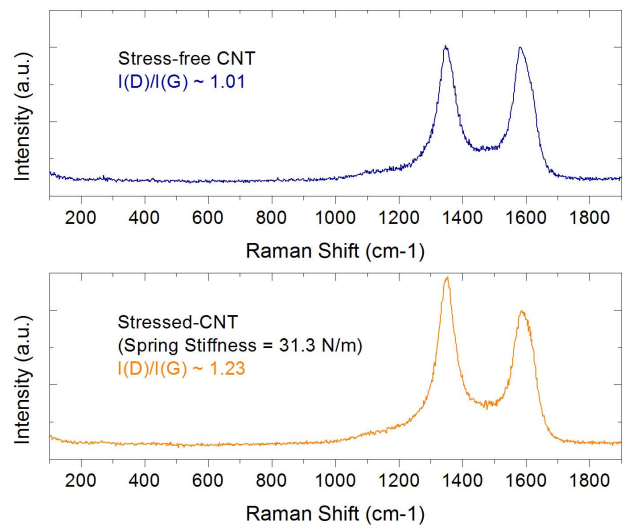


Figure 5: Raman spectra of the stress-free CNTs and stressed CNTs. When the CNTs were synthesized under compressive stress, the  $I(D)/I(G)$  ratio was increased indicating defectiveness increase.

micro-Raman spectroscopy with a 514 nm argon-ion laser illuminated on a spot of 1 μm in diameter in the middle of CNT arrays. The Raman spectra were obtained for the stress-free CNT array and the stressed CNT array (spring stiffness = 31.3 N/m) in Figure 3(b). As shown in Figure 5, the intensity ratio between the D- and G-band ( $I(D)/I(G)$ ) of stress-free CNTs was 1.01, and it increased abruptly to 1.23 when the CNTs were grown under compressive stress. The effect of compressive stress on the defectiveness and the resultant properties of CNT array will be further investigated in the future.

## CONCLUSIONS

In summary, we experimentally demonstrated length-controlled synthesis of CNT array using precisely adjusted and differently applied compressive forces by micromechanical springs during CVD process. When CNT array was grown under compressive stress, the CNTs were less-aligned and buckled, and as a result, the final length of CNT array decreased. This buckled morphology of the CNTs may have contributed to the increase of defectiveness inside the CNTs according to the Raman spectra analysis. Our approach to adjust the length of CNTs and the amount of internal defects could be applied to various MEMS devices which require aligned CNT arrays for advanced functionality.

## ACKNOWLEDGEMENTS

This research was supported by the Basic Science Research Program (2011-0002585) and the Fusion Research Program for Green Technologies (2011-0000005) through the National Research Foundation of Korea (NRF) funded by the Ministry of Education, Science and Technology, and by Korea Ministry of Environment as "Converging technology project" (2011-8-1565).

## REFERENCES

- [1] M.-F. Yu, O. Lourie, M. J. Dyer, K. Moloni, T. F.

- Kelly, R. S. Ruoff, "Strength and Breaking Mechanism of Multiwalled Carbon Nanotubes Under Tensile Load", *Science*, vol. 287, pp. 637-640, 2000.
- [2] T. W. Ebbesen, H. J. Lezec, H. Hiura, J. W. Bennett, H. F. Ghaemi, T. Thio, "Electrical Conductivity of Individual Carbon Nanotubes", *Nature*, vol. 382, pp. 54-56, 1996.
- [3] P. Kim, L. Shi, A. Majumdar, P. L. McEuen, "Thermal Transport Measurements of Individual Multiwalled Nanotubes", *Phys. Rev. Lett.*, vol. 87, 215502, 2001.
- [4] A. Cao, P. L. Dickrell, W. G. Sawyer, M. N. Ghasemi-Nejhad, P. M. Ajayan, "Super-Compressible Foamlike Carbon Nanotube Films", *Science*, vol. 310, pp. 1307-1310, 2005.
- [5] A. Peigney, Ch. Laurent, E. Flahaut, R. R. Bacsá, A. Rousset, "Specific Surface Area of Carbon Nanotubes and Bundles of Carbon Nanotubes", *Carbon*, vol. 39, pp. 507-514, 2001.
- [6] D. N. Futaba, K. Hata, T. Yamada, T. Hiraoka, Y. Hayamizu, Y. Kakudate, O. Tanaike, H. Hatori, M. Yumura, S. Iijima, "Shape-engineerable and Highly Densely Packed Single-walled Carbon Nanotubes and Their Application as Super-capacitor Electrodes", *Nature Mater.*, vol. 5, pp. 987-994, 2006.
- [7] J. Suhr, P. Victor, L. Ci, S. Sreekala, X. Zhang, O. Nalamasu, P. M. Ajayan, "Fatigue Resistance of Aligned Carbon Nanotube Arrays under Cyclic Compression", *Nature Nanotechnol.*, vol. 2, pp. 417-421, 2007.
- [8] A. Cao, V. P. Veedu, X. Li, Z. Yao, M. N. Ghasemi-Nejhad, P. M. Ajayan, "Multifunctional Brushes Made from Carbon Nanotubes", *Nature Mater.*, vol. 4, pp. 540-545, 2005.
- [9] G. Toth, J. Maklin, N. Halonen, J. Palosaari, J. Juuti, H. Jantunen, K. Kordas, W. G. Sawyer, R. Vajtai, P. M. Ajayan, "Carbon-Nanotube-Based Electrical Brush Contacts", *Adv. Mater.*, vol. 21, pp. 2054-2058, 2009.
- [10] J. Choi, J. Kim, "Batch-processed Carbon Nanotube Wall as Pressure and Flow Sensor", *Nanotechnology*, vol. 21, 105502, 2010.
- [11] D. N. Hutchison, N. B. Morrill, Q. Aten, B. W. Turner, B. D. Jensen, L. L. Howell, R. R. Vanfleet, R. C. Davis, "Carbon Nanotubes as a Framework for High-Aspect-Ratio MEMS Fabrication", *J. Microelectromech. Syst.*, vol. 19, pp. 75-82, 2010.
- [12] W. A. de Heer, A. Chatelain, D. Ugarte, "A Carbon Nanotube Field-Emission Electron Source", *Science*, vol. 270, pp. 1179-1180, 1995.
- [13] J. Choi, J.-I. Lee, Y. Eun, M.-O. Kim, J. Kim, "Microswitch with Self-assembled Carbon Nanotube Arrays for High Current Density and Reliable Contact", in *Proc. 24<sup>th</sup> Int. Conf. Micro Electro Mechanical Systems (MEMS 2011)*, Cancun, Mexico, January 23-27, 2011, pp. 87-90.
- [14] J. Choi, J.-I. Lee, Y. Eun, M.-O. Kim, J. Kim, "Aligned Carbon Nanotube Arrays for Degradation-Resistant, Intimate Contact in Micromechanical Devices", *Adv. Mater.*, vol. 23, pp. 2231-2236, 2011.
- [15] J.-I. Lee, Y. Song, H. Jung, J. Choi, Y. Eun, J. Kim, "Deformable Carbon Nanotube-Contact Pads for Inertial Micro-Switch to Extend Contact Time", *IEEE Trans. Ind. Electron.*, 2011. (Online published, doi: 10.1109/TIE.2011.2163918)
- [16] Y. Eun, J.-I. Lee, J. Choi, Y. Song, J. Kim, "Integrated Carbon Nanotube Array as Dry Adhesive for High-Temperature Silicon Processing", *Adv. Mater.*, vol. 23, pp. 4285-4289, 2011.
- [17] C. T. Wirth, C. Zhang, G. Zhong, S. Hofmann, J. Robertson, "Diffusion- and Reaction-Limited Growth of Carbon Nanotube Forests", *ACS Nano*, vol. 3, pp. 3560-3566, 2009.
- [18] D. B. Geohegan, A. A. Puzos, I. N. Ivanov, S. Jesse, G. Eres, J. Y. Howe, "In situ Growth Rate Measurements and Length Control During Chemical Vapor Deposition of Vertically Aligned Multiwall Carbon Nanotubes", *Appl. Phys. Lett.*, vol. 83, pp. 1851-1853, 2003.
- [19] A. J. Hart, A. H. Slocum, "Force Output, Control of Film Structure, and Microscale Shape Transfer by Carbon Nanotube Growth under Mechanical Pressure", *Nano Lett.*, vol. 6, pp. 1254-1260, 2006.
- [20] A. Cao, R. Baskaran, M. J. Frederick, K. Turner, P. M. Ajayan, G. Ramanath, "Direction-Selective and Length-Tunable In-Plane Growth of Carbon Nanotubes", *Adv. Mater.*, vol. 15, pp. 1105-1109, 2003.

## CONTACT

Jongbaeg Kim, School of Mechanical Engineering,  
Yonsei University, South Korea, tel: +82-2-2123-2812;  
[kimjb@yonsei.ac.kr](mailto:kimjb@yonsei.ac.kr)